The AAPS Journal (2019) 21: 33
DOI: 10.1208/s12248-019-0306-1

Research Article

A Density-Changing Centrifugation Method for Efficient Separation of Free Drugs from Drug-Loaded Particulate Delivery Systems

Lu Han,[1,2] Hongyan Zhan,[3] Xun Sun,[1] Zhi-Rong Zhang,[1] and Li Deng[1,4]

Received 9 November 2018; accepted 8 February 2019; published online 25 February 2019

Abstract. Commonly used separation techniques, such as ultracentrifugation, chromatography, and membrane separation, have inherent drawbacks that limit their usage. Herein, we introduced a new separation method, density-changing centrifugation (DCC), which is based on trisodium citrate (TC) and ultracentrifugation. Paclitaxel-loaded cationic solid lipid nanoparticles (SLNs/PTX) and doxorubicin-loaded PEGylated liposomes (Lipo/Dox) were prepared as model drug delivery particulates. After optimizing TC concentration and centrifugal conditions, DCC showed superior separation efficiency and accuracy over common ultracentrifugation and ultrafiltration methods and displayed comparable or even better separation efficiency compared with size-exclusion chromatography, as demonstrated by the determination of encapsulation efficiency, Tyndall effect, transmittance, and drug recovery. DCC was also proven to minimally impact the size distribution, surface morphology, and thermal properties of the nanoparticles and liposomes, and moreover, it did not affect the determination of drug concentrations. Together, DCC has been demonstrated as a neat and effective method for the separation of free drugs from drug-loaded SLNs and liposomes, which shall be of great benefit for the development of particulate based delivery systems.

KEY WORDS: density; encapsulation efficiency ; separation; trisodium citrate; ultracentrifugation.

INTRODUCTION

Particulate drug delivery systems including nanoparticles, liposomes, emulsions, microspheres, and cell membrane-derived particles are gaining increasing attentions among pharmaceutical scientists and medical doctors. Particulate drug delivery systems can be used in multiple fields, such as tumor therapy (1,2), imaging and diagnostics (3,4), immunoregulation (5,6), and nutrition supplement (7). Bioactive drugs or functional materials are most likely encapsulated in nano- or microparticles or adsorbed onto the surface of particulates to improve their pharmacokinetic profiles and avoid nonspecific distribution of free drugs (8,9). Usually, the encapsulation efficiency is one of the most important parameters to evaluate the quality of particulate formulations. However, the accurate determination of encapsulation efficiency depends on the complete separation of the entrapped drugs from the free drugs. Thus, the separation method can dramatically influence the accuracy of encapsulation efficiency determination, which may further impact the determination of drug dosage, as well as the pharmacokinetic profiles and pharmacological behavior *in vivo* (10,11).

The most commonly used separation technologies, including ultracentrifugation (12), chromatography (13), membrane separation (14), and magnetic separation method (15), have unique advantages that endow them with high separation effect; however, these methods suffer from inherent drawbacks that more or less limit their application. Ultracentrifugation has been developed into density gradient ultracentrifugation, viscosity gradient ultracentrifugation, and velocity gradient ultracentrifugation, which separate free drugs from particulates by using the differences of weight, density, or viscosity (16,17). Theoretically, ultracentrifugation is suitable for the precipitation of all particles that have different densities or viscosities than the liquid medium. However, the usage of ultracentrifugation is largely restricted, which requires expensive specialized centrifugal instrument that supports ultra-high centrifugal force. Also, ultracentrifugation needs a relatively long period of time that may lead to

Lu Han and Hongyan Zhan are co-first authors.

Electronic supplementary material The online version of this article (https://doi.org/10.1208/s12248-019-0306-1) contains supplementary material, which is available to authorized users.

[1] Key Laboratory of Drug Targeting and Delivery Systems, Ministry of Education, West China School of Pharmacy, Sichuan University, No 17, Section 3, Southern Remin Rd, Chengdu, 610041, China.
[2] College of Pharmacy, Southwest Minzu University, Chengdu, China.
[3] Chongqing YaoPharm Co., Ltd., 100 Xingguang Avenue, Renhe Town, Yubei District, Chongqing, China.
[4] To whom correspondence should be addressed. (e–mail: denglisunny@163.com)

1550-7416/19/0300-0001/0 © 2019 American Association of Pharmaceutical Scientists

drug leakage. Therefore, ultracentrifugation often leads to poor separation efficiency under generally acceptable operation conditions, especially when the density of particulates is similar to the liquid medium (10,18). Size-exclusion chromatography (SEC) is one of the most extensively used chromatography methods for separation, and the principle of SEC separation is based on the size differences between molecules and particles (19,20). However, SEC requires long elution time and large elution volume that may result in sample dilution. Moreover, SEC was blamed for poor recovery of the model drugs, and this might result in false measurement of encapsulation efficiency (10,21). Membrane separation methods, including ultrafiltration and dialysis, separate particulates of different sizes by the interception of the filter membrane (22). Membrane separation is simple, convenient, and practical, whereas the membrane is prone to adsorb drugs and particulates, as well as it may lead to the leakage of particulates into the filtrate (10). Therefore, alternative separation methods need to be developed to meet the requirements of various separation conditions.

In this study, we developed a rapid and convenient separation method density-changing centrifugation (DCC), which was inspired by density gradient ultracentrifugation, for effective separation of particulates. To measure the feasibility and effectiveness of DCC, solid lipid nanoparticles (SLNs) and liposomes, which are important and widely used preparations in researches, were taken as model particulates. SLNs were loaded with hydrophobic drug (paclitaxel, PTX), while liposomes were loaded with hydrophilic drug (doxorubicin hydrochloride, Dox). The separation efficiency was evaluated by encapsulation efficiency and Tyndall effect; the integrity of particulates was reflected by size distribution, surface charge, morphology, and thermal properties; additionally, the influence of DCC on the detection of drugs was demonstrated by the recovery of drugs in trisodium citrate (TC) solution. To the best of our knowledge, this is the first report of a novel separation method based on TC and centrifugation,

METHODS AND MATERIALS

Chemicals, Reagents, and Materials

Glyceryl monostearate (GMS) was purchased from Taiwei Pharmaceutical Co., Ltd. (Shanghai, China). Soy phosphatidylcholine (SPC, S100) and pegylated lipids (DSPE-PEG_{2000}) were purchased from Lipoid (Ludwigshafen, Germany). Dimethyldioctadecylammonium bromide (DDAB) and cholesterol (Chol) were obtained from Sigma-Aldrich (St. Louis, USA). Paclitaxel was obtained from Haoxuanbio. Co., Ltd. (Xian, China). Dox was obtained from Beijing HVSF United Chemical Materials Co., Ltd. (Beijing, China). Trisodium citrate was obtained from Jinshan Chemical Reagent Co., Ltd. (Chengdu, China). High-performance liquid chromatography (HPLC) grade methanol, acetonitrile, and triethylamine were obtained from Kemiou Chemical Reagent Co., Ltd. (Tianjin, China). Deionized water was acquired by an UPH water purification system (ULUPURE Ultrapure Technology, Chengdu, China). All other reagents were of analytical grade.

Preparation of PTX-loaded Nanoparticles and Dox-loaded Liposomes

PTX-loaded solid lipid nanoparticles were prepared using a film-ultrasonic method as previously described (23). Briefly, GMS (15 mg), SPC (15 mg), Chol (10 mg), DDAB (5 mg), and PTX (1 mg) were dissolved in chloroform and evaporated to form a thin film, and SLNs/PTX were obtained after sonication (80 W, 60 s) with 5 mL of deionized water. Blank nanoparticles were prepared in the absence of PTX.

Dox-loaded liposomes were prepared using a transmembrane pH-gradient method with some modifications (24). Briefly, SPC (60 mg), Chol (20 mg), and DSPE-PEG_{2000} (20 mg) were dissolved in chloroform and evaporated to form a thin film, and the film was hydrated with 6 mL of pre-warmed citrate buffer (100 mM, pH 3.6) at 37°C for 1 h. The resulting liposomal suspension was homogenized by sonication (120 W, 60 s), followed by adjusting the pH to 7.4 by adding sodium carbonate solution (240 mM, pH 11.4). Subsequently, 0.4 mL of Dox solution (5 mg/mL) was mixed with the liposome sample and incubated in the water bath at 60°C for 1 h. The Lipo/Dox was obtained after the mixture cooled down. To prepare blank liposomes, 0.4 mL of deionized water without Dox was used to mix with the liposome sample.

Density-Changing Centrifugation

Firstly, the amount of TC added, the centrifugal time and rotational speed should be screened to optimize the separation conditions. The prepared nanoparticles and liposomes were mixed with different concentrations of TC solution (pH 6.5 for SLNs/PTX and pH 7.2 for Lipo/Dox) to make the final TC concentration from 0 to 20% (*m*/*v*). Afterwards, the mixtures were centrifuged at 4°C for different centrifugal time and at different rotational speed to separate free drugs from nanoparticles. After centrifugation, the drug-loaded nanoparticles or liposomes floated to the uppermost layer, and the free drugs precipitated to the bottom or remained in the middle liquid layer. Subsequently, the middle liquid layer was extracted carefully by a syringe, and the absorbance (A) at 550 nm was measured using a UV spectrophotometer (Varian, USA). Transmittance (*T*%) was calculated to determine the separation efficiency and to obtain the optimized TC concentration and centrifugal conditions.

$$T\% = 10^{-\mathrm{A}(550\ \mathrm{nm})} \times 100$$

For detection of encapsulation efficiency, 2 mL of freshly prepared SLNs/PTX or Lipo/Dox was mixed with 2 mL of optimized TC solution, followed by centrifuging at the selected centrifugal conditions, and the drug-loaded particles were collected from the upper solid layer and dissolved in the elution solvent and subjected to HPLC analysis.

Ultracentrifugation

Common ultracentrifugation was used to separate free drugs from encapsulated drugs (12). Two milliliter of freshly prepared Lipo/Dox were mixed with 2 mL of citrate diluent

(if it is not explained elsewhere, citrate diluent and the external water phase of liposomes contained the same salt concentration and pH value) or 2 mL of freshly prepared SLNs/PTX were mixed with 2 mL of water, and the mixtures were centrifuged at 40000 rpm at 4 °C for 40 min and 120 min or at the optimized centrifugal conditions selected for DCC. After centrifugation, the supernatant was collected carefully for the measurement of Tyndall effect and transmittance (550 nm), and the drug-loaded particles precipitated in the bottom were dissolved in solvent for HPLC analysis.

Size-Exclusion Chromatography

Drug-loaded particles were separated from free drugs by Sephadex G-50 chromatography (21). The activated gel in a glass column was equilibrated by eluent (water for SLNs and citrate diluent for liposomes), and then saturated with blank liposomes or nanoparticles. After loading the particulate samples, the eluents of purified particulates were collected by monitoring the absorbance at 254 nm. After dissolved in the elution solvent, the content of drugs encapsulated in particulates was determined by HPLC.

Ultrafiltration

The non-entrapped drugs in the outer aqueous phase of particulates were separated by the ultrafiltration method (10). Lipo/Dox and SLNs/PTX were diluted twice with citrate diluent and water respectively, and the diluted samples were centrifuged at 3000×*g* for 30 min in ultrafiltration tubes (10 KD, Millipore, USA), and then the filtrates were collected for the measurement of Tyndall effect and transmittance (550 nm) or collected into volumetric flasks and dissolved in the elution solvent for HPLC analysis.

Determination of Encapsulation Efficiency by HPLC

Free PTX, purified SLNs/PTX, and initial SLNs/PTX were dissolved and disrupted in methanol and analyzed by an Agilent 1200 HPLC system (Agilent, USA) (23). A Kromasil ODS-1 C_{18} column (150 × 4.6 mm, 5 μm) was used, and the mobile phase consisted of 55% (*v*/*v*) acetonitrile and 45% (*v*/*v*) purified water. The flow rate was set at 1.0 mL/min, the column temperature was maintained at 35 °C, and the detection wavelength was 227 nm.

Free Dox and encapsulated Dox were dissolved in ethanol containing 1% hydrochloric acid and analyzed by Agilent 1200 HPLC system (Kromasil ODS-1 C_{18} column (150 × 4.6 mm, 5 μm) (10). Thirty percent (*v*/*v*) acetonitrile and 70% (*v*/*v*) purified water (containing 0.2% (*v*/*v*) triethylamine, pH 4.0) were used as mobile phase. Flow rate, 1.0 mL/min; column temperature, 35°C; and wavelength, 253 nm.

For the method of DCC, common ultracentrifugation and size exclusion chromatography, the encapsulation efficiency (%) = weight of drug in SLNs or in liposomes/weight of the feeding drug; and for the method of ultrafiltration, encapsulation efficiency (%) = (weight of the feeding drug −weight of drug in filtrate)/weight of the feeding drug.

Recovery of Drugs in TC Solution

The recovery of PTX in TC solution was measured by adding known amounts of PTX stock solution into methanol aqueous solution containing 10% (*m*/*v*) TC (pH 6.5), leading to a theoretical PTX concentration of 3.65, 14.20, and 24.34 μg/mL. The recovery of Dox in TC solution was conducted by mixing known amounts of Dox stock solution with 20% TC solution (pH 7.2), and the final concentration of Dox was adjusted to 3.86, 13.82, and 27.25 μg/mL by adding ethanol containing 1% hydrochloric acid. The samples were centrifuged at 5000 rpm for 10 min and the supernatant was filtered through a 0.22 μm membrane and analyzed using HPLC. The drug recovery (%) = measured drug concentration/theoretical drug concentration.

Measurement of Physicochemical Characteristics

The physicochemical properties of SLNs/PTX and Lipo/Dox under different conditions were characterized in terms of size distribution, zeta potential, morphology, and thermal properties. Conditions included the initial state, mixed state (particulates mixed with a certain amount of TC), and recovered state (particulates recovered from the upper solid layer after the optimal DCC). The recovered SLNs/PTX was obtained by dispersing the upper solid layer in water and adding a few drops of 20% (*m*/*v*) citric acid to deflocculate, followed by sonication (80 W, 60 s). The recovered Lipo/Dox was acquired by dispersing the upper solid layer in citrate diluent followed by sonication (80 W, 30 s).

The hydrodynamic size, polydispersity index (PDI), and zeta potential of the SLNs/PTX and Lipo/Dox in the above three states were measured in triplicate by photon correlation spectroscopy (PCS) (Malvern Zetasizer Nano ZS90, UK). SLNs/PTX was diluted by water, while Lipo/Dox was diluted by citrate diluent.

The morphology of SLNs/PTX and Lipo/Dox in different states was observed using an H-600 transmission electron microscopy (TEM, Hitachi, Japan) after negative staining with 1% phosphotungstic acid (pH 6.5) as described previously (23).

Differential scanning calorimetry (DSC) was performed on a DSC analyzer (Netzsch DSC 200 PC, Germany) to investigate the thermal properties of the samples (23). SLNs/PTX and Lipo/Dox in three states were lyophilized separately, and the dried samples in addition to PTX, Dox and TC were sealed individually in the aluminum crimp cell, and heated from 0 to 300°C at a rate of 10°C/min under nitrogen atmosphere.

Statistical Analysis

Statistical analyses were performed using GraphPad Prism software (San Diego, CA, USA). Differences between two groups were evaluated for significance using the unpaired Student's *t* test, while one-way ANOVA followed by Tukey's multiple comparisons test was used for multiple comparisons. All quantitative data were expressed as the mean ± standard deviation (SD). Levels of significant differences were expressed as follows: $*p < 0.05$, $**p < 0.01$, $***p < 0.001$, $****p < 0.0001$.

RESULTS

Optimized Density-Changing Centrifugation

Common ultracentrifugation precipitates the particulates by means of density differences between the particulates and the liquid medium (18). However, the density of particulates such as liposomes and nanoparticles is very close to the density of liquid medium. Therefore, common ultracentrifugation often drives the particulates incompletely to the bottom of the centrifuge tube (10,18) (Fig. 1). In contrast to common ultracentrifugation, SLNs/PTX and Lipo/Dox flocculated after mixed with a certain amount of TC solution, and the particle solution turned to three separated layers after DCC: the lighter particulates floated to the topside to form the upper solid layer, the soluble free drugs (Dox) dissolved in TC solution, and remained in the middle liquid layer while the insoluble drug crystals (PTX) precipitated in the bottom (Fig. 1). On the other hand, no PTX "precipitate" was detected on the top of the liquid after PTX suspension (1 mg of PTX powder was added into 3 mL of water and dispersed by sonication) was mixed with 10% TC and centrifuged at 40000 rpm for 40 min (data not shown), indicating that the presence of free PTX would not interfere with the separation effect of DCC.

Then, the transmittance of the middle liquid layer after DCC was calculated to determine the separation efficiency, and the higher transmittance showed the higher separation efficiency. As shown in Fig. 2, the transmittance of the supernatant of SLNs increased as the concentration of TC solution increased (Fig. 2 a); however, the transmittance of the supernatant of liposomes decreased when the concentration of TC solution reached to 5% and 10% as compared with 0% TC solution (Fig. 2 d). In order to figure out this difference, we measured the density range of SLNs/PTX and Lipo/Dox using density gradient centrifugation. In sucrose density gradient centrifugation, liposomes were mainly distributed in the range of 0–20% (1.0000–1.0813 g/cm^3) sucrose solutions (Fig. S1A), while in TC density gradient centrifugation, liposomes were mainly distributed in the layer of 5% TC solution (1.0302 g/cm^3) (Fig. S1C), indicating that the density of untreated liposomes was lower than the density of 15% TC solution (1.0890 g/cm^3), while it was close to the density of 5% TC solution when contacted with 5% TC. Therefore, when mixed with 0% TC (Fig. 2 d), most liposomes precipitated after centrifugation due to their higher density than the medium. However, the bulk liposomes remained in the liquid after centrifugation when mixed with 5% or 10% (1.0605 g/cm^3) TC solution, probably because that their density was close to the density of 5% and 10% TC solutions, and liposomes were less flocculated in low concentration of TC solution. Therefore, the transmittance of the supernatant of liposomes in 5% and 10% TC solution was lower than that in 0% TC solution. Nevertheless, when the concentration of TC solution increased to 15% or 20% (1.1168 g/cm^3), liposomes flocculated more heavily, and the density difference between the liposomes and TC solution increased, resulting in the rise of liposomes and the increase of transmittance of middle liquid layer after centrifugation. On the other hand, SLNs were mainly distributed in the range of 0–10% (1.0000–1.0367 g/cm^3) sucrose solutions (Fig. S1B), while in TC gradient centrifugation, they could be flocculated in large quantities and distributed above the 5% TC solution (Fig. S1D), indicating that flocculation could improve the centrifugal separation effect. Therefore, when mixed with 5% TC, most SLNs got flocculated and floated upwards due to their lower density than the medium, leading to improved transmittance than the group of 0% TC (Fig. 2 a). Moreover, when mixed with 10% TC, almost all the SLNs floated to the topside after centrifugation and the transmittance of the middle liquid layer was nearly to 100% (Fig. 2 a), probably due to the increased density difference between the severely flocculated SLNs and the TC solution. In summary, for the separation of cationic SLNs/PTX, the optimal final concentration of TC was 10% (*m*/*v*) (Fig. 2 a), the optimal centrifugal time was 20 min (Fig. 2 b), and rotational speed was 20,000 rpm (Fig. 2 c); for the separation of Lipo/Dox, the optimal final concentration of TC was 20% (*m*/*v*) (Fig. 2 d), centrifugal time was 10 min (Fig. 2 e), and rotational speed was 20,000 rpm (Fig. 2 f). These optimal separation conditions for DCC were used in the following sections, unless otherwise noted.

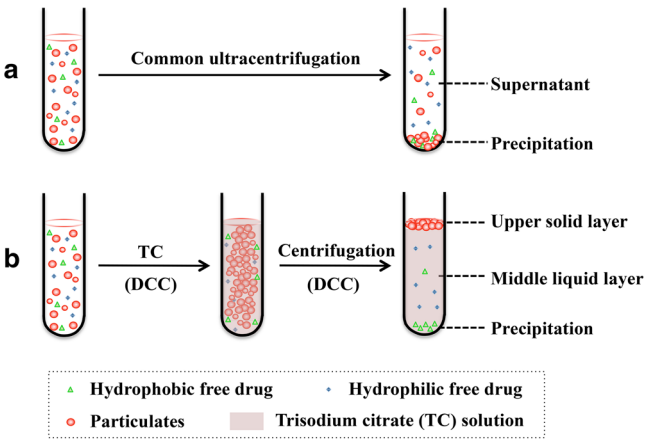

Fig. 1. Schematic diagram of common ultracentrifugation (**a**) and DCC (**b**). During DCC, particulates (SLNs/PTX and Lipo/Dox) flocculated when mixed with a certain concentration of TC solution, and by means of the density difference with TC solution, particles floated upwards to form the upper solid layer after centrifugation

Comparison of the Separation Effect

In order to evaluate the separation effect of DCC, encapsulation efficiency of the particulates was measured by HPLC, and the Tyndall effect and transmittance of the liquid after separation were compared respectively.

As shown in Fig. 3 a–b, in group of DCC, the free drugs were easily separated from the particulates after centrifugation at low rotational speed and short time, and the encapsulation efficiency of SLNs/PTX (Fig. 3 a) and Lipo/Dox (Fig. 3 b) was 96.50 ± 3.52% and 95.26 ± 0.70%, respectively. However, the common ultracentrifugation groups were failed to efficiently separate drug-loaded particles from preparations and resulted in low encapsulation efficiency, even in intense centrifugal conditions (40,000 rpm and 120 min). These results indicated that DCC had excellent

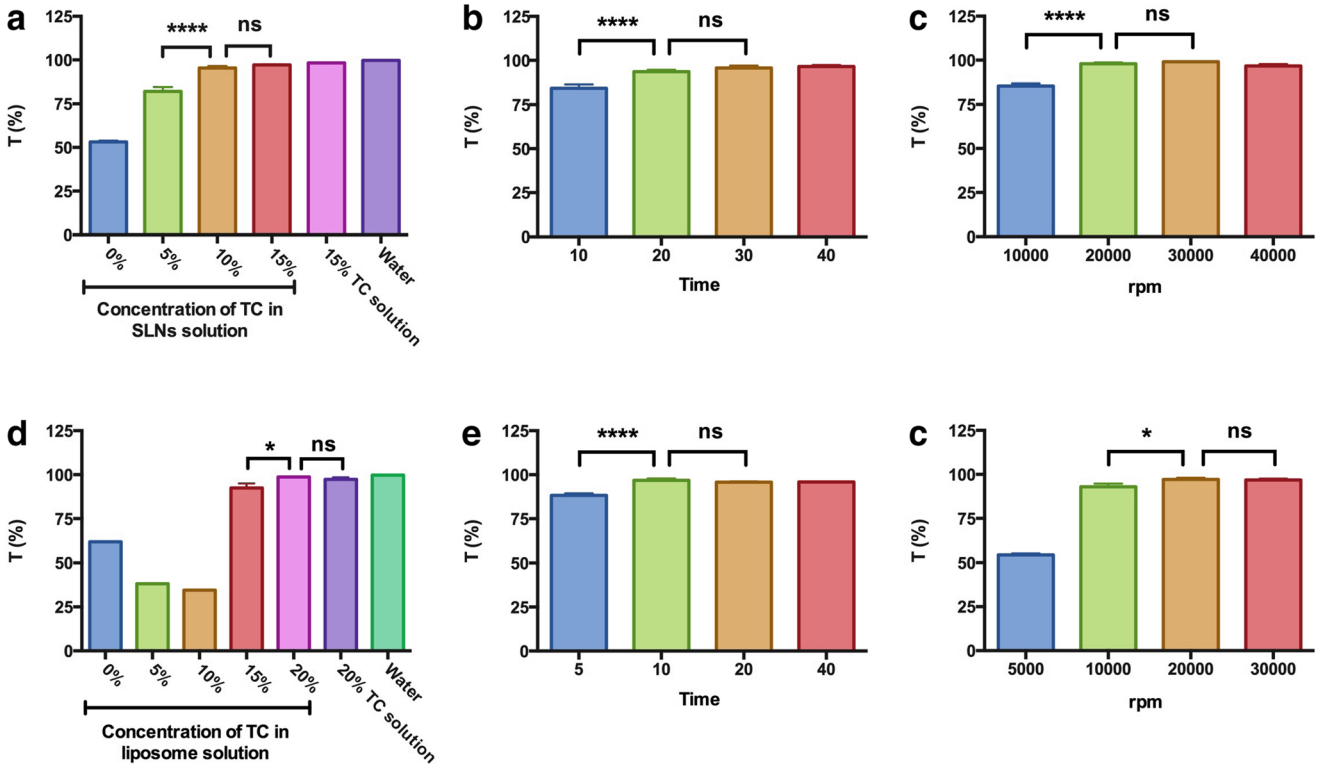

Fig. 2. Optimal separation conditions of DCC. Samples were mixed with different concentrations of TC, followed by centrifuging at different centrifugal conditions, and the absorbance (550 nm) of the middle liquid layer was measured by UV spectrophotometer to calculate the transmittance. (**a**–**c**) Influence of TC (**a**, 40000 rpm, 90 min), centrifugal time (**b**, 10% TC, 40000 rpm), and rotational speed (**c**, 10% TC, 20 min) on the separation of SLNs/PTX. **d**–**f** Influence of TC (**d**, 40000 rpm, 90 min), centrifugal time (**e**, 20% TC, 20000 rpm), and rotational speed (**f**, 20% TC, 10 min) on the separation of Lipo/Dox. Fifteen percent TC solution (**a**), 20% TC solution (**d**), and water (**a** and **d**) were negative controls without SLNs/PTX or Lipo/Dox. Data are shown as mean ± SD ($n = 3$), *$p < 0.05$, ****$p < 0.0001$; ns, not significant

separation effect, saved a great deal of time and reduced centrifugal costs.

SEC is regarded as the most widely used method for the purification of nanoparticles and liposomes (13,19,20,25), thus the Sephadex G-50 chromatography was used as the positive control for separation. As shown in Fig. 3 a–b, the encapsulation efficiency of SLNs/PTX in DCC group was significantly higher than that of Sephadex G-50 group, while the encapsulation efficiency of Lipo/Dox in two groups had no significant difference. In order to figure out whether SLNs were suspected of adsorbing PTX, we mixed free PTX with freshly prepared blank SLNs (1 mg PTX in 5 mL solution), and all the separated layers (the upper solid layer, middle liquid layer, and precipitation) after DCC were collected for the detection of adsorbed PTX. This result showed that the upper solid layer contained 8.14 ± 0.22% of total PTX, and no drug was detectable in the middle liquid layer, while 86.47 ± 1.37% of total PTX was found in precipitation. Therefore, we concluded that SLNs would adsorb very small amount of PTX, and the vast majority PTX would precipitate to the bottom after DCC. In a word, DCC had comparable separation effect with SEC for the separation of liposomes, and it was much more suitable for the separation of cationic solid lipid nanoparticles.

Ultrafiltration is suitable for the separation of water-soluble drugs from drug-loaded particles. However, the free drugs are easily adsorbed and retained on the ultrafiltration membrane (26), resulting in reduced concentration of filtered free drugs and false positive value of encapsulation efficiency. As shown in Fig. 3 a, the encapsulation efficiency of SLNs/PTX in the groups of DCC (96.50 ± 3.52%) and ultrafiltration (100.54 ± 0.64%) had no significant difference, probably because the encapsulation efficiency was too high to show the difference. However, the recovery of PTX solution filtrated by ultrafiltration was nearly 0% (Supplementary Table I). Therefore, ultrafiltration is not suitable for the separation of hydrophobic PTX, because the insoluble PTX crystals tend to be trapped by the filter membrane, resulting in false encapsulation efficiency. As shown in Fig. 3 b, the encapsulation efficiency of Lipo/Dox in ultrafiltration group was significantly higher than that of DCC group, implying that most free Dox was adsorbed by ultrafiltration membrane, and this adsorption was further proved by the low recovery of Dox solution filtrated by ultrafiltration (Supplementary Table II). Therefore, DCC was superior to ultrafiltration for the separation of free drugs from PTX-loaded SLNs and Dox-loaded liposomes.

Tyndall effect was used to display the separation effect of DCC more intuitively, and the transmittances of "free drug solution" separated by different methods were measured to further compare the separation effects. As shown in Fig. 3 c–d, different states of SLNs/PTX (Fig. 3 c) and Lipo/Dox (Fig. 3 d) displayed different light effects after irradiated by a red laser. Both of the freshly prepared particulates (Fig. 3 c1, d1) and particulates after common ultracentrifugation (40,000 rpm, 40 min, Fig. 3 c3, d3) showed an obvious light beam, and the

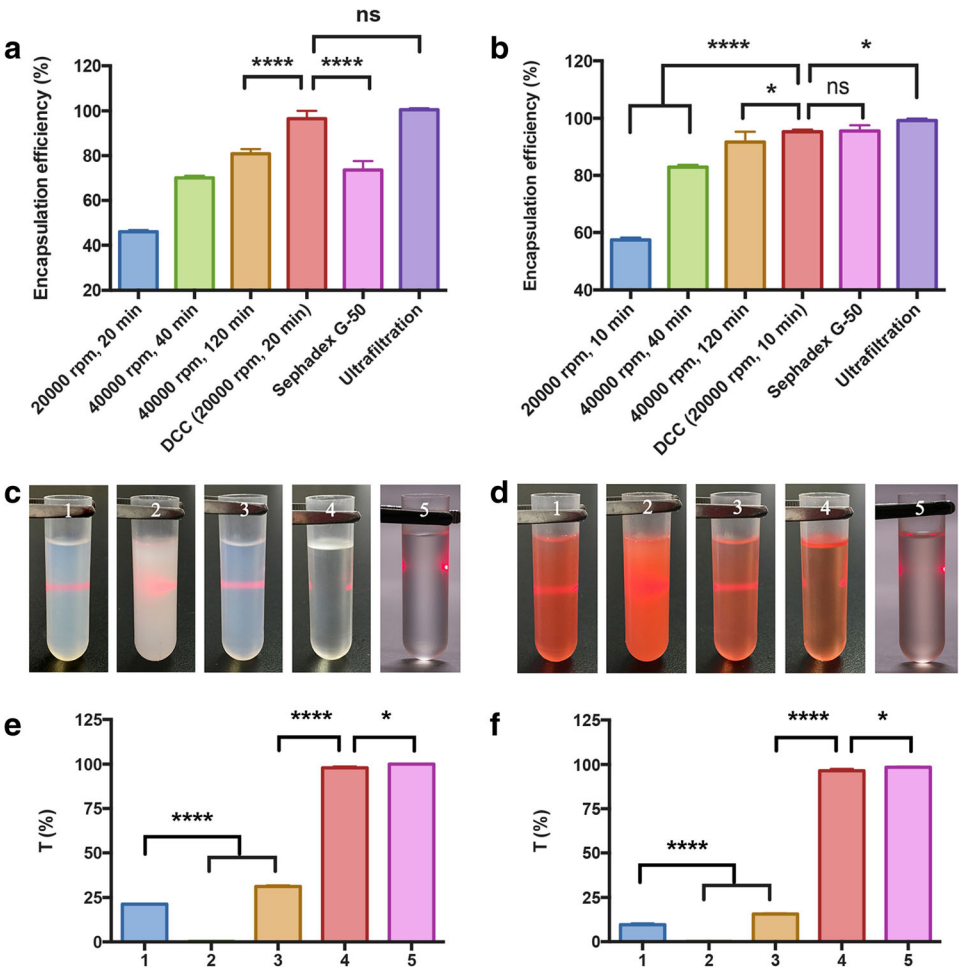

Fig. 3. DCC separated the free drugs and particulates efficiently. **a**–**b** Encapsulation efficiency of PTX in SLNs (**a**) and Dox in liposomes (**b**) was determined by HPLC. Free drugs were separated from particulates by different methods: common ultracentrifugation, DCC (10% TC, 20000 rpm, 20 min for SLNs/PTX; 20% TC, 20000 rpm, 10 min for Lipo/Dox), Sephadex G-50 chromatography and ultrafiltration. **c**–**f** Tyndall effect of SLNs/PTX (**c**) and Lipo/Dox (**d**) and transmittance (A_{550nm}) of SLNs/PTX (**e**) and Lipo/Dox (**f**) before and after common ultracentrifugation, DCC and ultrafiltration: 1, freshly prepared particulates; 2, particulates mixed with TC; 3, samples after common ultracentrifugation (40,000 rpm, 40 min); 4, samples after the optimal DCC; 5, filtrates after ultrafiltration. Data are shown as mean ± SD ($n = 3$), *$p < 0.05$, ****$p < 0.0001$; ns, not significant

transmittances of these samples were significantly lower than that of the DCC group (Fig. 3 e–f), indicating that the common ultracentrifugation was failed to precipitate the particulates completely and there still existed a large number of particulates in the supernatant. When particulates were mixed with TC (Fig. 3 c2, d2, e2, and f2), the scattered light in the turbid dispersion system and the extremely low transmittance reflected the aggregation of particulates. However, after optimal DCC (Fig. 3, c4, d4, e4, and f4), the particulates floated to the topside, and the missing light beam in the middle liquid layer and the high transmittance indicated that the separation was quite complete and few particulates remained in the liquid. Although the filtrates of ultrafiltration (Fig. 3, c5, d5) showed no obvious light beams in the tubes, and the transmittance was significantly higher than that of the DCC group (Fig. 3 e–f), these results might also be false positive results that caused by the adsorption or interception of free drugs by the ultrafiltration membrane.

To sum up, DCC was proven to have excellent separation efficiency. The drug-loaded particles and free drugs showed varying behaviors after DCC: the former floated to the top, while the latter remained in the liquid or precipitated to the bottom of the centrifuge tube.

Recovery of Drugs in TC Solution

In order to evaluate the influence of TC on the detection of drugs, Dox and PTX were mixed with a certain amount of TC, and the recovery of drugs was measured by HPLC. The recovery rates of PTX (Table I) and Dox (Table II) in low, middle, and high concentrations were higher than or equal to 95%, and the RSD values were less than 1.86% ($n = 3$). These results indicated that the "density changer" (TC) was harmless to the quantitative detection of PTX and Dox.

Table I. Recovery of PTX in 10% TC Solution ($n = 3$)

C_{added} (μg/mL)	$C_{measured}$ (μg/mL)	Recovery (%)	RSD (%)
3.65	3.76 ± 0.06	103.01 ± 1.63	1.59
14.20	13.49 ± 0.21	94.98 ± 1.55	1.61
24.34	24.25 ± 0.05	99.62 ± 0.18	0.18

Size and Surface Morphology

To investigate the integrity of particulates after DCC, the size distribution, surface charge, and morphology of particulates in different states were measured. As shown in Fig. 4, the size and PDI of nanoparticles were increased sharply after mixing with 10% TC, showing an obvious aggregation according to TEM; however, the zeta potential of nanoparticles in the mixed state was dramatically decreased from 55.37 ± 0.70 mV to 8.91 ± 0.54 mV, resulting in the reduction of repelling forces between particulates, therefore leading to aggregation. After optimized DCC, the nanoparticles were dispersed again by "deflocculant" (citrate) and short sonication: the size, zeta potential, and morphology of nanoparticles (SLNs/PTX after DCC) recovered to the levels of initial state, while PDI decreased from 0.26 ± 0.02 to 0.17 ± 0.02, probably due to the final sonication and deflocculant. These results indicated that the integrity of nanoparticles was intact after DCC that was suitable for the separation of cationic SLNs.

Characterizations of Lipo/Dox were shown in Fig. 5. Similar to the changes of SLNs/PTX, the aggregated liposomes resulted in increased size and PDI after mixed with 20% TC, and then the size, PDI, and morphology of liposomes restored to the initial levels after DCC and sonication. However, zeta potential of liposomes remained stable under all circumstances. These results indicated that the integrity of Lipo/Dox was unaffected after DCC, and the aggregation of liposomes did not rely on the changes of zeta potential.

Overall, DCC is proven to separate the cationic SLNs and PEGylated liposomes efficiently without impairing the integrity of particulates. Moreover, the size distribution, surface charge, and morphology could return to the original states.

Differential Scanning Calorimetry Analysis

Differential scanning calorimetry (DSC) is used as a useful tool to study the thermal properties of nanoparticles and liposomes, which provides detailed information on the stability and relevant physicochemical properties of the drugs within particulate formulations (23,27). As shown in Fig. 6 a, in the temperature range of 200 to 250°C, the endothermic peak and exothermic peak in the thermogram of PTX were absent in the thermogram of SLNs/PTX, indicating that the PTX was likely to be dispersed molecularly in the lipid matrix. Due to the low percentage of SLNs/PTX as compared with TC, the thermogram of the mixture (SLNs/PTX mix 10% TC) overlapped with the thermogram of TC. However, the thermogram of recovered SLNs/PTX after optimal DCC (SLNs/PTX after DCC) was consistent with the thermogram of SLNs/PTX, indicating that the PTX-loaded SLNs were stable and remained intact during the process of DCC. Similar to the changes of SLNs/PTX, the thermograms in Fig. 6 b showed that Dox was dispersed molecularly in the liposomes and the Dox-loaded liposomes remained undamaged after DCC.

Based on the results of DSC, size distribution, and surface morphology, DCC had no impact on the physicochemical properties of nanoparticles and liposomes, and this novel separation method might be suitable for the separation of other particulate formulations from free drugs.

Table II. Recovery of Dox in 20% TC Solution ($n = 3$)

C_{added} (μg/mL)	$C_{measured}$ (μg/mL)	Recovery (%)	RSD (%)
3.86	3.82 ± 0.02	99.11 ± 0.46	0.47
13.82	13.87 ± 0.22	100.37 ± 1.63	1.62
27.25	27.88 ± 0.52	102.33 ± 1.91	1.86

DISCUSSION

Ultracentrifugation separates free drugs from particulates by using the differences of weight, density, or viscosity (16,17). However, the density of particulates such as liposomes and nanoparticles is very close to the density of liquid medium, resulting in inadequate separation and a waste of time (10,18). Moreover, common ultracentrifugation precipitates the particulates and insoluble drug crystals together, thus it cannot tell the difference between the encapsulated drugs and insoluble free drugs, leading to wrong result of encapsulation efficiency. In contrast to common ultracentrifugation, DCC is performed by dissolving a certain amount of TC in the liquid to sharply increase the density of liquid medium, as demonstrated by the comparison of the density difference between particulates and TC solutions (Fig. S1), thus the particulates turn to be much lighter than the liquid. In this condition, the particulates and free drugs would experience different destinies after DCC: the lighter particulates floated to the topside of the centrifuge tube, while the free drugs remained in the liquid (the free hydrophilic Dox dissolved in the liquid) or precipitated in the bottom (the unencapsulated poorly soluble PTX could precipitate after ultracentrifugation) (Fig. 1). Therefore, the reversed and increased density difference between the particulates and liquid medium is the main reason for the high separation efficiency of DCC.

DCC method depends on the combination of TC and ultracentrifugation, and therefore the concentration of TC and the centrifugal conditions should be optimized first to achieve the best separation performance. The transmittance of colloidal solution is usually low due to the large quantity of particulates, and the transmittance will increase if the particulates are removed by centrifugation. Therefore, transmittance was used to reflect the separation efficiency of DCC. For the particulates with different surface properties and densities, the separation conditions should be optimized individually, because the lower concentration of TC or lower centrifugal time and speed could lead to incomplete

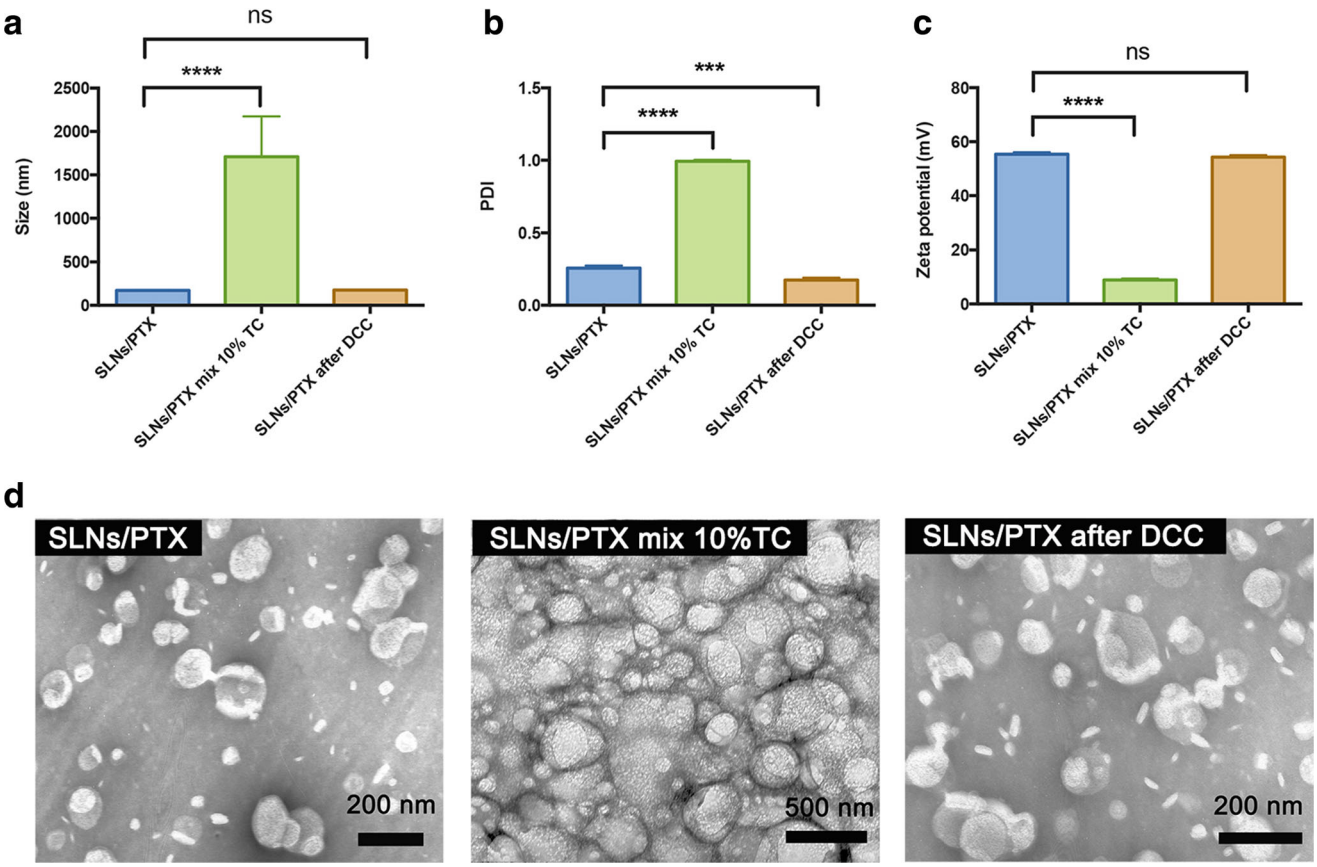

Fig. 4. Characterizations of SLNs/PTX in different states. The size (**a**), PDI (**b**), and zeta potential (**c**) of samples were measured by dynamic light scattering, and the surface morphology (**d**) of samples was visualized by TEM. SLNs/PTX: freshly prepared PTX-loaded SLNs; SLNs/PTX mix 10% TC: the mixture of SLNs/PTX and 10% (*m*/*v*) TC; SLNs/PTX after DCC: the recovered SLNs/PTX from the upper solid layer after optimal DCC (10% TC; 20,000 rpm; 20 min). Data are shown as mean ± SD ($n = 3$), ***$p < 0.001$, ****$p < 0.0001$; ns, not significant

separation and incompact particle layer, while the higher separation conditions would result in waste and even drug leakage.

The separation of free drugs and drug-loaded particles plays a crucial part in the accurate detection of encapsulation efficiency. In other words, inaccurate encapsulation efficiency caused by poor separation may misguide the screening of formulations and even lead to wrong drug dosage (10,11). Then, we compared the separation effect of DCC with three other commonly used separation methods (common ultracentrifugation, SEC, and ultrafiltration) by measuring the encapsulation efficiency, Tyndall effect, and the transmittance. All the results in Fig. 3 displayed much better separation efficiency of DCC than that of common ultracentrifugation. These results further confirmed that the reversed and widened density difference between the particulates and liquid medium could greatly benefit the separation efficiency of DCC. The ultrafiltration membrane may adsorb free drugs (Dox) and particulates (26), and it could also trap the insoluble free PTX, resulting in low drug recovery and inflated value of encapsulation efficiency. Therefore, DCC was also superior to ultrafiltration for the separation of free drugs from Dox-loaded liposomes and PTX-loaded SLNs. However, as compared with SEC, DCC showed comparable encapsulation efficiency for the detection of Lipo/Dox, while it showed much higher encapsulation efficiency for the detection of SLNs/PTX. We first excluded the possibility that cationic SLNs could adsorb partial free PTX to compromise the accuracy of encapsulation efficiency measurement. Therefore, the problem might lay in the Sephadex G-50 chromatography. It was reported that SEC exhibited good separation, but it also suffered from low recovery (10,21). There was a great possibility that the separation mechanism of Sephadex G-50 for the separation of PTX and SLNs consisted of two patterns: adsorption and molecular sieve (28). Therefore, a part of cationic SLNs could be adsorbed and retained on the Sephadex gel filler, leading to low encapsulation efficiency. While DCC did not encumber the floating of SLNs, thus the encapsulation efficiency was much closer to the true value.

The most crucial part that impacts the practicability of DCC is the influence of additives on the detection of drugs. The recovery assays of Dox and PTX in TC solution indicated that the "density changer" (TC) did not affect the determination of drug concentrations. It is very important to note that the pH of TC aqueous solution is slightly alkaline, while some drugs (such as PTX) are unstable in such alkaline environment (29), thus, the pH of TC solution should be adjusted to the most suitable pH of drug to prevent drug degradation or precipitation.

Furthermore, maintaining the integrity of particles is another important prerequisite for a good separation method. However, both the turbidity of particulate solutions after mixing with TC and the agglomerate of particulates after

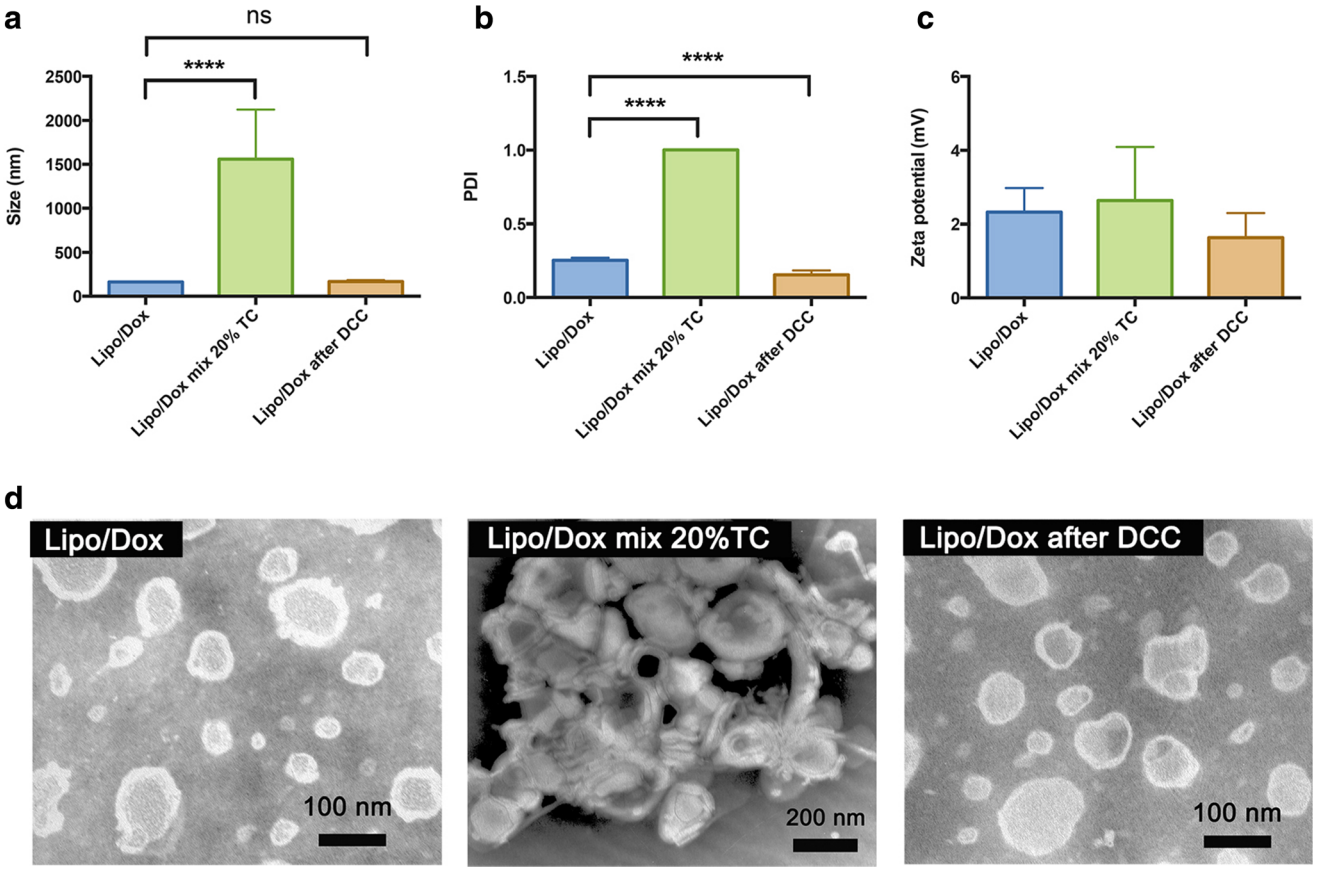

Fig. 5. Characterizations of Lipo/Dox in different states. The integrity of Lipo/Dox was determined by measuring the size (**a**), PDI (**b**), zeta potential (**c**), and the surface morphology (**d**). Lipo/Dox: freshly prepared Dox-loaded liposomes; Lipo/Dox mix 20% TC: the mixture of Lipo/Dox and 20% (*m*/*v*) TC; Lipo/Dox after DCC: the recovered Lipo/Dox from the upper solid layer after optimal DCC (20% TC; 20,000 rpm; 10 min). Data are shown as mean ± SD ($n = 3$), ****$p < 0.0001$; ns, not significant

centrifugation probably meant the disruption of particulates. Fortunately, according to the results of size distribution, surface morphology, and DSC analysis (Figs. 4, 5, and 6), DCC had minimal impact on the physicochemical properties of particulates. Moreover, the size distribution, surface charge, and morphology could return to the original states after proper treatment. For example, after DCC, SLNs/PTX could be restored to the original states by adding some citrate and short sonication. Therefore, the citrate played a dual role in the flocculation and dispersion of SLNs. In the beginning, the TC neutralized the surface charge of nanoparticles and reduced the repelling force between particulates, resulting in the flocculation of nanoparticles; after DCC, the addition of citrate could adhere to the particulates and increase the zeta

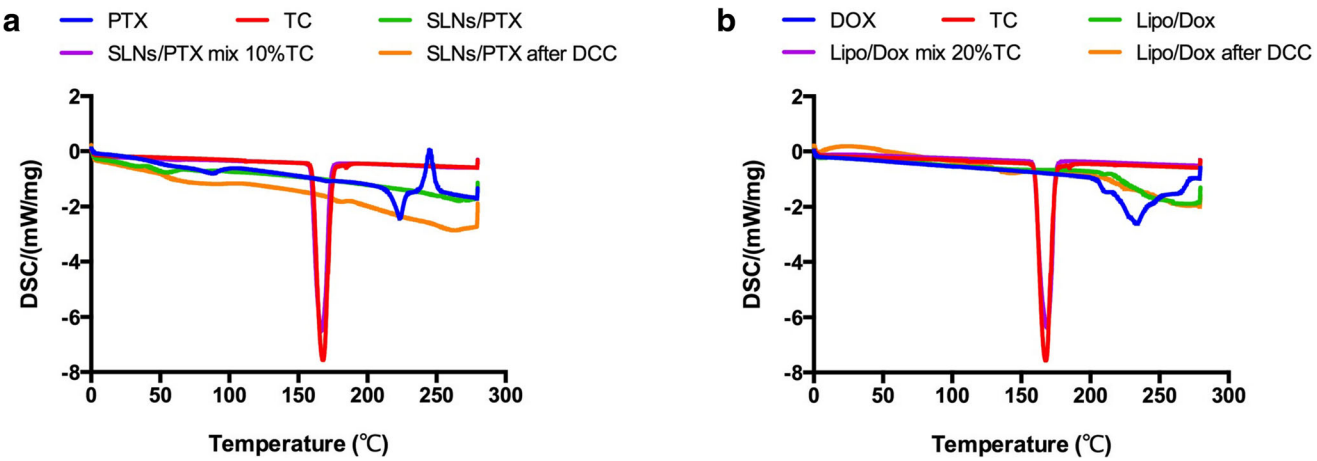

Fig. 6. DSC thermograms of samples. **a** DSC thermograms of PTX, TC, initial SLNs/PTX, SLNs/PTX mixed with 10% TC, and the recovered SLNs/PTX after optimal DCC (SLNs/PTX after DCC). **b** DSC thermograms of Dox, TC, original Lipo/Dox, Lipo/Dox mixed with 20% TC, and the recovered Lipo/Dox after optimal DCC (Lipo/Dox after DCC)

potential, thereby leading to the re-dispersion of nanoparticles. On the other hand, the high concentration of TC might compress the surface PEG hydration layer of liposomes, leading to reduced steric hindrance that further caused the aggregation of Lipo/Dox. However, the exact mechanism for the flocculation of PEGylated liposomes and cationic SLNs needs to be explored further.

Agents (citrate, tartrate, phosphate, etc.) that can reverse the charge to cause flocculation can theoretically be used to separate the particulates. However, if the agents only cause flocculation without inversely increasing the density difference, the flocculated nanoparticles will still precipitate to the bottom of the centrifuge tube, making it impossible to distinguish the encapsulated drug from the precipitated free drug. Moreover, if the agents can only increase the density difference without causing flocculation, then more severe centrifugation conditions are required to achieve satisfied separation effect. Therefore, DCC separated the SLNs/PTX and Lipo/Dox efficiently from free drugs by two main mechanisms: inversely increasing the density difference between particulates and liquid medium, and causing reversible flocculation of particulates. However, for other particulates, such as normal Dox-loaded liposomes (phospholipid: cholesterol = 4: 1, without PEG layer), no flocculation was observed when the liposomes were mixed with TC, and more intense centrifugal conditions (40,000 rpm and 90 min) were needed to achieve efficient separation, thus the separation mechanism might only contain increased density difference. Therefore, the separation mechanism of DCC for different drug-loaded particulates may be varied and the inherent and detailed mechanisms for the efficient separation of DCC should be explored in greater depth.

Although DCC showed superior separation effect for cationic SLN/PTX and PEGylated Lipo/Dox, the following possible limitations of DCC should be noticed. DCC may be not suitable for the separation of drugs that are electrostatically adsorbed on the surface of the particulates, because the high concentration of TC may change the surface charge of particulates, thereby resulting in dissociation of drugs and particulates. Moreover, the addition of high concentration of TC may increase the osmolarity of solution, leading to structural changes of some particulates, especially for the liposomes. In this article, even if the concentration of TC was up to 20%, there was no obvious drug leakage during DCC and the structure of liposomes was intact, which was demonstrated by the high encapsulation efficiency of Lipo/Dox determined by DCC method and the recoverable size, PDI, and morphology of liposomes after DCC. However, the impact of higher concentration of TC on the integrity of liposomes needs to be further investigated. Furthermore, the optimization processes of DCC should be performed separately for each specific nanodelivery system. Especially for the particulates that cannot cause flocculation when mixed with TC, intense centrifugal conditions are also required to achieve satisfactory separation effect. Finally, in addition to SLNs/PTX and Lipo/Dox, more particulate formulations (such as emulsions, micelles, polymeric nanoparticles, inorganic nanoparticles, and albumin nanoparticles) and more kinds of drugs (such as proteins, peptides, and nucleic acid drugs) should be investigated to verify the feasibility of DCC.

CONCLUSION

A simple and efficient separation method based on TC and ultracentrifugation was developed and validated for the rapid separation of free drugs from PTX-loaded SLNs and Dox-loaded liposomes. By means of reversed density difference and reversible flocculation, DCC can separate the drug-loaded particles efficiently without impairing the integrity of particulates. Together, our results highlighted the feasibility and potential of using DCC for the rapid separation of either hydrophilic or hydrophobic drugs from nanoparticles and liposomes, which may show applicability in the pharmaceutical industry.

FUNDING INFORMATION

The authors are grateful for the financial support from the National Natural Science Foundation of China (81690261).

Publisher's Note Springer Nature remains neutral with regard to jurisdictional claims in published maps and institutional affiliations.

REFERENCES

1. Yi X, Lian X, Dong J, Wan Z, Xia C, Song X, et al. Co-delivery of pirarubicin and paclitaxel by human serum albumin nanoparticles to enhance antitumor effect and reduce systemic toxicity in breast cancers. Mol Pharm. 2015;12(11):4085–98.
2. Zanganeh S, Hutter G, Spitler R, Lenkov O, Mahmoudi M, Shaw A, et al. Iron oxide nanoparticles inhibit tumour growth by inducing pro-inflammatory macrophage polarization in tumour tissues. Nat Nanotechnol. 2016;11(11):986–94.
3. Rao L, Bu LL, Cai B, Xu JH, Li A, Zhang WF, et al. Cancer cell membrane-coated upconversion nanoprobes for highly specific tumor imaging. Adv Mater. 2016;28(18):3460–6.
4. Tasciotti E, Liu X, Bhavane R, Plant K, Leonard AD, Price BK, et al. Mesoporous silicon particles as a multistage delivery system for imaging and therapeutic applications. Nat Nanotechnol. 2008;3(3):151–7.
5. He C, Duan X, Guo N, Chan C, Poon C, Weichselbaum RR, et al. Core-shell nanoscale coordination polymers combine chemotherapy and photodynamic therapy to potentiate checkpoint blockade cancer immunotherapy. Nat Commun. 2016;7:12499.
6. Saravana KA, Ramaswamy NM. Chitosan microspheres as potential vaccine delivery systems. Int J Drug Delivery. 2011;3(1):43–50.
7. Weiss J, Decker EA, Mcclements DJ, Kristbergsson K, Helgason T, Awad T. Solid lipid nanoparticles as delivery systems for bioactive food components. Food Biophys. 2008;3(2):146–54.
8. Bose RJ, Lee SH, Park H. Biofunctionalized nanoparticles: an emerging drug delivery platform for various disease treatments. Drug Discov Today. 2016;21(8):1303–12.
9. Parveen S, Misra R, Sahoo SK. Nanoparticles: a boon to drug delivery, therapeutics, diagnostics and imaging. Nanomedicine. 2012;8(2):147–66.
10. Lv Y, He H, Qi J, Lu Y, Zhao W, Dong X, et al. Visual validation of the measurement of entrapment efficiency of drug nanocarriers. Int J Pharm. 2018;547(1–2):395–403.

11. Wallace SJ, Li J, Nation RL, Boyd BJ. Drug release from nanomedicines: selection of appropriate encapsulation and release methodology. Drug Deliv Transl Res. 2012;2(4):284–92.
12. Laouini A, Koutroumanis KP, Charcosset C, Georgiadou S, Fessi H, Holdich RG, et al. pH-sensitive micelles for targeted drug delivery prepared using a novel membrane contactor method. ACS Appl Mater Interfaces. 2013;5(18):8939–47.
13. Gao D, Tang S, Tong Q. Oleanolic acid liposomes with polyethylene glycol modification: promising antitumor drug delivery. Int J Nanomedicine. 2012;7:3517–26.
14. Liu Z, Zhu Y-Y, Li Z-Y, Ning S-Q. Evaluation of the efficacy of paclitaxel with curcumin combination in ovarian cancer cells. Oncol Lett. 2016;12(5):3944–8.
15. Elizarova IS, Luckham PF. Layer-by-layer encapsulated nano-emulsion of ionic liquid loaded with functional material for extraction of Cd 2+ ions from aqueous solutions. J Colloid Interface Sci. 2017;491:286–93.
16. Sun X, Tabakman SM, Seo WS, Zhang L, Zhang G, Sherlock S, et al. Separation of nanoparticles in a density gradient: FeCo@C and gold nanocrystals. Angew Chem Int Ed Eng. 2009;48(5):939–42.
17. Qiu P, Mao C. Viscosity gradient as a novel mechanism for the centrifugation-based separation of nanoparticles. Adv Mater. 2011;23(42):4880–5.
18. Ohnishi N, Tanaka S, Tahara K, Takeuchi H. Characterization of insulin-loaded liposome using column-switching HPLC. Int J Pharm. 2015;479(2):302–5.
19. Pellequer Y, Ollivon M, Barratt G. Methodology for assaying recombinant interleukin-2 associated with liposomes by combined gel exclusion chromatography and fluorescence. J Chromatogr B. 2003;783(1):151–62.
20. Zhang H, Zhang FM, Yan SJ. Preparation, *in vitro* release, and pharmacokinetics in rabbits of lyophilized injection of sorafenib solid lipid nanoparticles. Int J Nanomedicine. 2012;7:2901–10.
21. Guan P, Lu Y, Qi J, Niu M, Lian R, Wu W. Solidification of liposomes by freeze-drying: the importance of incorporating gelatin as interior support on enhanced physical stability. Int J Pharm. 2015;478(2):655–64.
22. Akthakul A, Hochbaum AI, Stellacci F, Mayes AM. Size fractionation of metal nanoparticles by membrane filtration. Adv Mater. 2005;17(5):532–5.
23. Shi S, Han L, Deng L, Zhang Y, Shen H, Gong T, et al. Dual drugs (microRNA-34a and paclitaxel)-loaded functional solid lipid nanoparticles for synergistic cancer cell suppression. J Control Release. 2014;194:228–37.
24. Li X, Hirsh DJ, Cabral-Lilly D, Zirkel A, Gruner SM, Janoff AS, et al. Doxorubicin physical state in solution and inside liposomes loaded via a pH gradient. BBA-Biomembranes. 1998;1415(1):23–40.
25. Ji P, Yu T, Liu Y, Jiang J, Xu J, Zhao Y, et al. Naringenin-loaded solid lipid nanoparticles: preparation, controlled delivery, cellular uptake, and pulmonary pharmacokinetics. Drug Des Devel Ther. 2016;10:911–25.
26. Mayer LD, St.-Onge G. Determination of free and liposome-associated doxorubicin and vincristine levels in plasma under equilibrium conditions employing ultrafiltration techniques. Anal Biochem 1995;232:149–157.
27. Demetzos C. Differential scanning calorimetry (DSC): a tool to study the thermal behavior of lipid bilayers and liposomal stability. J Liposome Res. 2008;18(3):159–73.
28. Gelotte B. Studies on gel filtration : sorption properties of the bed material sephadex. J Chromatogr A. 1960;3(1):330–42.
29. Amini-Fazl MS, Mobedi H, Barzin J. Investigation of aqueous stability of taxol in different release media. Drug Dev Ind Pharm. 2014;40(4):519–26.